Paste 2026 – AB Fourie, M Horta, M Oliveira & S Wilson (eds)

doi:10.36487/ACG_repo/2655_35

Structured experiments: the first step toward selecting tailings dewatering and filtration systems based on 2 decades of continuous data collection in Iran

Seyed Alireza Aghili [a,b], Shahram Hashemi Marghzar [a,*], Behnaz Mirshekari [a], Nader Montazerin [b]

[a] *Amatis Rabin Consulting Engineers, Islamic Republic of Iran*

[b] *Department of Mechanical Engineering, Amirkabir University of Technology, Islamic Republic of Iran*

Abstract

This study compiles and analyses over 2 decades of tailings sedimentation and filtration data from multiple mining operations in Iran, aiming to generalise empirical findings and improve comparability. Samples are classified into ferrous and non-ferrous tailings. Standardised procedures characterised particle size distribution (PSD), chemical composition (X-ray fluorescence), and specific gravity, followed by sedimentation and filtration tests to evaluate thickening, water recovery, and energy demand.

Pressure filtration was conducted under high- and low-pressure recessed chambers and membrane filtration, examining cake blow and core blow effects. Coarser tailings (D_{80} > 150 µm) showed steep settling and filtration responses with lower hydrodynamic resistance, while finer tailings (D_{80} < 100 µm) formed stable sediment structures with slower filtration.

Mineralogy significantly influenced behaviour: higher Fe_2O_3/Fe and lower SiO_2 promoted early aggregation and higher initial filtration rates in non-ferrous tailings, whereas higher SiO_2 increased porosity and cumulative filtrate, particularly in ferrous tailings. Silica effects varied with particle size, affecting pore structure and water release. Overall, the study provides an experimental basis for assessing tailings dewatering performance across a wide range of textural and mineralogical conditions.

Keywords: *tailing sedimentation experiment, tailing filtration experiment, weighted distribution index, X-ray fluorescence*

1 Introduction, variability of tailings and the requirement for systematic data acquisition

Mineral processing operations inherently face variability in ore mineralogy and texture, which causes pronounced fluctuations in tailings behaviour during solids–liquid separation stages such as sedimentation and filtration. These variations can impair equipment performance, lower recycled water quality, and increase operational costs. To address this, systematic characterisation of tailings through integrated datasets – encompassing chemical composition (X-ray fluorescence [XRF]), particle size distribution (PSD), sedimentation, and filtration behaviour – is essential for process optimisation and predictive modelling. This study analyses multi-source industrial datasets from various Iranian mineral plants to identify the governing parameters of tailings dewaterability. By correlating physicochemical properties with settling and filtration responses, it establishes an empirical framework for evaluating dewatering efficiency, offering a data-driven basis for designing and optimising tailings management systems.

* Corresponding author. Email address: marghzar@yahoo.com

2 State of knowledge on tailings dewatering and characterisation

2.1 Key factors and data-driven mechanistic insights into slurry sedimentation

Li & van Zyl investigated the sedimentation and separation behaviour of copper tailings, emphasising the influence of particle size and composition on settling dynamics. Using a zone-formation differential settling model, they conducted sequential and intermittent sedimentation tests on 6 suspensions with solids concentrations of 30–50 wt%. The results showed that coarse particles settled rapidly and accumulated at the column base, while fine particles remained suspended in the upper layers; with increasing solids concentration, the velocity contrast diminished and particle segregation became less distinct. Analysis of particle distribution profiles revealed that conventional models capture only part of the observed behaviour and must be refined to include aggregation effects, particle morphology, and wall interactions. Overall, coarse particle settling was identified as the dominant mechanism governing separation, and the study recommended treating fine particles with similar velocities as a single representative group to enhance model simplicity and predictive accuracy (Li & van Zyl 2024a).

Li & van Zyl conducted column-settling experiments on copper tailings to study particle concentration and mudline evolution. Settling strongly depends on particle size distribution, interparticle interactions, and mineralogy. Higher fine-particle content reduces settling rate, thickens the compacted layer, and stabilises the suspension, while a clear interface forms between supernatant and solids. The study highlights that initial solids concentration and hydrodynamic forces primarily govern settling dynamics and suspension stability, critical for tailings dam design, recycled water management, and filtration optimisation (Li & van Zyl 2024b).

Wang et al. studied ultrafine tailings sedimentation and thickening at lab and semi-industrial scales to optimise flocculant type, dosage, and slurry concentration. Using a high-molecular-weight flocculant at 50 g/t and 8% feed concentration, they achieved a maximum underflow solids of 59.5%, while overdosing reduced efficiency by limiting particle bridging. Lower solids flux, reduced flocculant use, and greater bed height improved underflow concentration. Three thickening regimes – continuous feeding, dynamic equilibrium, and bed descent – were identified, with bed descent showing lower underflow due to shorter compression. Predictive models linking bed height to underflow provide practical strategies for ultrafine tailings thickening control (Wang et al. 2025).

Paoli & da Silveira studied the settling behaviour of iron tailings from Brazil's Fundão dam using Tanfloc, a bio-based tannin polymer, as an alternative to inorganic coagulants. A full factorial design tested pH (6–8) and coagulant concentration (5–15 g/L) on sedimentation. pH had little effect, while higher Tanfloc concentrations significantly reduced supernatant turbidity and improved phase separation. An exponential model best described the data, showing distinct differences between iron-bearing and non-ferrous tailings. Under optimal conditions, clarified and settled phase concentrations were 12.9 and 263.5 g/L, respectively, with a separation efficiency of 65.6% (Paoli & da Silveira 2023).

Sadangi et al. studied the sedimentation of iron tailings rich in goethite and kaolinite. Settling velocity decreases sharply with increasing solids, from ~2 m/h at 10% solids to 0.24 m/h at 35%. An anionic flocculant improves sedimentation: 10 g/t suffices at 10% solids, but 60 g/t is needed at 30%, and beyond 30% the rate remains low even with flocculant. Experiments also show that pH ~5 gives optimal settling without reagent. The study highlights that proper flocculant dosing and pH control are essential for ultrafine iron ore sedimentation (Sadangi et al. 2020).

Han et al. investigated the settling of ultrafine iron ore tailings from the Daye mine, China, addressing low settling rates and high flocculant consumption in backfill operations. They studied flocculant type and dosage, pulp concentration, and stirring time. Optimal conditions – an anionic flocculant at 30 g/t, 0.3% concentration, and >45 min mixing – yielded a maximum settling rate of 8.2 mm/min and underflow solids of ~58%. Microscopy showed flocs with lowest porosity (32.65%), highest fractal dimension (1.914), and compact uniform structure. Floc size increased from 10.55 μm at the top to 38.79 μm at the bottom, indicating gradual compression and dewatering. The study highlights that proper flocculant selection and mixing significantly improve sedimentation efficiency and backfill quality (Han et al. 2022).

Tan et al. studied factors controlling sedimentation rate, focusing on flocculant dosage, floc structure, and fractal characteristics. Denser flocs with lower porosity and smaller pores settle faster, while fine particles (<20 μm) increase drag and stabilise the suspension, and coarse particles support overall settling. Higher fractal dimensions indicate compact, stable flocs, improving packing. Greater solids–liquid density contrast enhances settling via buoyancy. As bed depth increases, flocs enlarge and densify due to compression, expelling interstitial water and accelerating sedimentation (Tan et al. 2022).

In summary, tailings sedimentation and thickening are mainly governed by particle size distribution, solids concentration, mineralogy, and aggregation. Coarse particles dominate initial settling, while fine fractions and high-solids content slow settling by increasing hydrodynamic resistance and suspension stability. Flocculant-assisted sedimentation can enhance dewatering, but its efficiency depends strongly on mineralogy and operating conditions. Despite this, systematic experimental studies linking particle size and Fe–Si composition to both sedimentation and filtration remain limited, motivating the present work.

2.2 Approaches to monitoring and data acquisition in pressure filtration and analysis

Fränkle et al. studied copper tailings filtration, focusing on filtration pressure, air-blow, and cake thickness effects. Increasing pressure slightly reduces residual moisture, showing low compressibility, while post-filtration air blowing significantly lowers water content and saturation, though some pores retain water. Cakes of 40 and 55 mm take longer to reach equilibrium as thickness increases, but final moisture and mechanical properties are similar. Effective dewatering requires balancing cohesion for geotechnical stability and low adhesion for easy detachment. Optimised air-blow pressure and duration yield a stable, brittle, and easily detachable cake (Fränkle et al. 2024).

In another study, the same researchers developed a combined filtration–shear testing apparatus to quantitatively evaluate adhesion and cohesion in iron tailings (D_{80} = 38.2 μm, density = 3,050 kg/m³) under pressures of 250 and 1,250 kPa, using polypropylene, nylon, and felt filter media. The results show that higher filtration pressure and air blowing both reduce cake moisture and proportionally increase mechanical strength: when moisture drops below 20 wt%, adhesive shear strength ($\tau_{(Cloth)}$) rises by about 4–5 kN/m², and cohesive strength ($\tau_{(Cake)}$) increases by roughly 2 kN/m². The ratio $\sigma_{(Cake)}/\sigma_{(Cloth)}$ = 1.15, and the critical ratio $\tau_{(Cake)}/\sigma_{(Cake)} > 17.4$ ensures shear stability. Increasing pressure from 250 to 1,250 kPa approximately doubles adhesion strength for polypropylene cloth and enhances internal cohesion by about 1.5 times, confirming the strong coupling between filtration pressure, residual moisture, and mechanical integrity of the filter cake (Fränkle et al. 2022).

Hassan introduced the High-Pressure Dewatering Roller (HPDR) Mark-II as an alternative to filter presses for copper and nickel tailings. Initial tests on copper tailings, with or without flocculant, produced cakes with 83.1% solids, matching filter press performance. After mechanical improvements, nickel tailings reached 87.9% solids at 7 MPa and low roller speed. Solid throughput was 302 kg/m²·h for nickel and 73 kg/m²·h for copper, demonstrating that HPDR can achieve filter-press-level efficiency in continuous operation (Hassan et al. 2025).

Nopehewa et al. conducted filtration experiments on 2 mineral tailings at 0.2, 0.4, and 0.6 MPa to develop an empirical predictive model. Individual and mixed particle size fractions were tested for porosity, specific cake resistance, final moisture, and surface area. Particles finer than 15 μm increased resistance and slowed filtration, while coarser fractions improved drainage. Nearly linear correlations between fine-particle content and porosity, moisture, and surface area enabled a linear model to predict filtration behaviour of new mixtures. Optimising particle size distribution, particularly by removing some particles <15 μm, significantly enhances filtration efficiency and reduces dewatering costs (Nopehewa et al. 2023).

Kaswalder et al. examined the air-blowing stage of copper sulfidic tailings filtration to evaluate the effects of air-blow duration and intensity on final moisture and thixotropic behaviour. Experiments on 2 tailings types – one from a gold carbon-in-pulp circuit – were performed in a laboratory filter press at 10 bar with air-blowing times of 100, 150, and 300 seconds. For highly permeable tailings, extending air blowing to 300 seconds significantly reduced moisture, eliminated thixotropy, and produced stable, solid cakes.

In contrast, fine-grained and clay-rich cakes showed minimal moisture reduction and remained unstable due to low air permeability. The study found that particle size distribution and mineralogy govern air-blowing efficiency: fine particles and clays (<20 μm) block airflow and impede drainage. Additionally, longer, low-rate air blowing proved more effective than short, high-pressure bursts, as excessive velocities create preferential channels that lower overall drying efficiency (Kaswalder & Hawkey 2023).

Cacciuttolo Vargas et al. examined the dewatering behaviour of mineral tailings through laboratory filtration tests, showing that performance is governed by particle size distribution, mineralogy, and slurry microstructure. Results from constant-pressure and continuous filtration experiments indicate that although increasing pressure reduces final cake moisture, at high-solids concentrations the specific cake resistance becomes the dominant limiting factor. Fine particles (<20 μm) significantly increase resistance and lower permeability, whereas reducing this fraction markedly enhances filtration efficiency. The application of high-molecular-weight polymeric flocculants produces more open, porous cake structures that improve filtrate flow. During air blowing, extended duration and reduced airflow rates are most effective for highly permeable cakes but have negligible impact on fine-grained, low-permeability materials. Overall, the study emphasises that effective selection and optimisation of dewatering technologies – such as filter presses and HPDR – require comprehensive physicochemical characterisation and performance-based laboratory validation for each specific tailings type (Cacciuttolo Vargas & Pérez Campomanes 2022).

Diaz et al. conducted laboratory and pilot-scale studies at the Ada Tepe gold mine, Bulgaria to assess the technical and economic feasibility of implementing a tailings filtration system. Tests on thickened tailings with 57 wt% solids revealed that the high proportion of fine particles (<10 μm, over 40%) significantly extends the filtration cycle. Pressure filtration experiments showed that producing a stable, transportable cake requires achieving a final solids content of about 84 wt% (Diaz et al. 2023).

Luo et al. showed at industrial-scale that clay minerals, especially kaolinite, strongly limit tailings filtration and dewatering. Clay-rich tailings increase filtration time and required filter area, reducing dewatering capacity, raising energy consumption, and increasing maintenance. The platy structure and high aspect ratio of clay particles create densely packed networks with fine pores and tortuous flow paths, decreasing permeability and increasing hydraulic resistance, so filtration rates remain low even under high pressure (Luo et al. 2024).

Olcay et al. evaluated filtration and dewatering of ultrafine phosphate tailings, identifying chamber thickness, feed pressure, and cycle time as key factors. For fine tailings (<70 μm), increasing feed pressure up to 7 bar reduced cake moisture and improved initial filtration, though overall performance remained below industrial targets. Using hydrated lime as a filter aid enhanced floc formation, increased cake permeability, and lowered filtrate turbidity below 100 NTU, but high reagent demand raised costs and introduced variability in recycled water (Olcay et al. 2025).

In summary, previous studies show that mineral tailings dewatering is mainly controlled by particle size distribution, mineralogy, filtration pressure, and air blowing. Fine particles and clay minerals increase cake resistance and reduce permeability, limiting pressure filtration and air-blowing efficiency, while coarser fractions enhance drainage and cake stability. Higher filtration pressures and optimised air blowing can lower residual moisture and improve mechanical integrity, but benefits are material-dependent and constrained by cake microstructure. Comparative experimental frameworks systematically linking particle size and mineralogy to filtration efficiency and energy demand remain limited, highlighting the need for generalised, data-driven assessments like the present study.

2.3 Comparative insights into slurry classification through settling and pressure filtration metrics

Ferreira et at. demonstrate that the sedimentation behaviour of various suspensions – including mineral, chemical, and industrial or municipal waste water – can be accurately modelled using the Weibull distribution function with only 2 key parameters: the shape and scale factors. This model effectively describes settling dynamics over a wide range of sedimentation rates and shows superior performance compared with

exponential or power-law models, particularly in capturing concentration–time relationships at engineering scales (Ferreira et al. 2021).

Hernández et al. investigate paste slurries derived from copper tailings (Collahuasi mine, Chile) and iron tailings (Ourocom Plant, Brazil) and demonstrate that the pronounced differences in density (1.5 times higher for iron) and particle size (6.5 versus 45 μm) are the primary factors controlling the contrasting rheological and flow behaviours of the 2 pastes. The finer-grained iron tailings reach the paste state more rapidly but exhibit lower flowability, with an angle of repose of approximately 11°, compared with 15° for the copper paste. Rheologically, the copper paste shows stable thixotropic behaviour across all concentrations and is more suitable for pumping, whereas the iron paste displays a combination of thixotropic and rheopectic characteristics that make transport more challenging (Hernández et al. 2009).

Pham et al. employ a high-pressure Nutsche filtration system to evaluate the dewatering performance of various mineral materials, including apatite and copper concentrates, fine coal tailings, and bauxite residue (red mud). The results show that filtration efficiency is primarily governed by particle morphology and mineralogical composition. Samples of apatite and copper, characterised by uniform cubic particles, form homogeneous and permeable filter cakes with low specific resistance in the range of 1.5×10^{-13} to 2.5×10^{-12} m^{-2} and achieve final moisture contents between 15 and 20%. In contrast, fine-grained materials such as coal and red mud, composed of platy or clay-rich particles, tend to block filter pores, resulting in high specific resistance values up to 10^{13} m^{-2} and elevated residual moisture levels of 25–35% (Pham et al. 2024).

Collectively, the reviewed studies show that mineral tailings dewatering behaviour depends on particle size distribution, mineralogy, and operating conditions. In sedimentation, coarse particles accelerate settling while fine ones stabilise the suspension; higher solids concentrations lead to more uniform settling. In filtration, particle shape dominates – angular grains form permeable cakes with low moisture (≈15–20%), whereas platy or clay-rich particles cause pore blockage and higher moisture (≈25–35%). Given this variability, the present study compiles 2 decades of data from Iranian mineral plants to systematically evaluate the key factors controlling sedimentation and filtration performance.

3 Data acquisition and processing of slurry characteristics

3.1 Methodological framework of the study

The present study analyses 4 categories of experimental datasets from various mineral processing plants to investigate tailings dewatering: PSD, chemical analysis (XRF), sedimentation tests, and filtration tests. Data from multiple Iranian processing units are examined to identify empirical patterns that can predict tailings dewaterability and guide optimal process strategies. PSD and XRF data are first analysed independently to understand their roles in tailings' rheological and hydrodynamic behaviour. Subsequently, sedimentation and filtration results are treated as dependent variables to evaluate their relationships with the patterns derived from PSD and XRF analyses.

3.2 Study on tailing particle size distribution pattern

3.2.1 Conventional classification of particle size distribution

This section analyses the PSD of various mineral tailings samples (Figure 1). To better interpret particle behaviour in sedimentation and filtration, the PSD is divided into functional ranges: very fine particles (1–30 μm), which settle poorly and require flocculation; fine-to-medium particles (30–75 μm), the most influential range for thickening and filtration; semi-coarse particles (75–150 μm), representing a transition zone between colloidal and granular behaviour; and coarse particles (>150 μm), which settle almost instantly and are easily retained by filters (Tchobanoglus et al. 2003; Pham 2005).

This empirical classification has key limitations: it is qualitative, lacks a numerical index for statistical comparison, neglects continuous PSD variation and overlap between size intervals, and cannot isolate the effects of multi-stage grinding.

3.2.2 Definition of weighted distribution index based on 2 log-normal modelling of particle size distribution

PSD fitting analysis shows that, due to multi-stage crushing, grinding, and classification, many datasets cannot be accurately represented by a single log-normal function. A dual log-normal model better captures 2 dominant particle populations without distorting the overall distribution. This is especially evident in the Talashgaran Phase 2 sample, where combining 2 log-normal components is necessary to reproduce observed size characteristics. Compared with a single log-normal, the dual model more effectively reflects multi-stage grinding, recirculating loads, and coexistence of coarse and fine fractions. For consistency across datasets, a unified PSD descriptor (Equation 1) is introduced as a representative parameter. Table 1 summarises fitting coefficients and weighting factors, and subsequent analyses use this standardised criterion. This index, referred to as the weighted distribution index (WDI), represents the weighted cumulative function of the dual log-normal distribution and quantitatively expresses the cumulative proportion of particles finer than a specified reference diameter.

$$WDI = W_1\Phi\left(\frac{\ln(di-\mu_1)}{\sigma_1}\right) + W_2\Phi\left(\frac{\ln(di-\mu_2)}{\sigma_2}\right) \qquad \text{WDI configuration (1)}$$

The WDI quantitatively represents the fraction of particles smaller than a reference diameter, weighted by the relative contribution of each log-normal component, thereby integrating both the dispersion and representative size of particles into a single, dimensionless criterion. Physically, a lower WDI corresponds to a coarser nominal particle size. In the WDI formulation, d_i denotes the process threshold or reference diameter, while μ and σ define the modal position and spread of each log-normal component, and the weighting coefficient w specifies its relative contribution to the overall PSD. This index effectively retains the precision of dual log-normal modelling while providing a unified, comparable, and physically interpretable parameter for ranking particle size behaviour across different mineral samples. The process threshold d_i is determined analytically by evaluating the variance of cumulative passing values across samples, where the diameter corresponding to maximum variance represents the most discriminative size for comparative analysis. Consequently, the WDI offers a robust framework for linking PSD characteristics to industrial processes such as sedimentation, filtration, and hydrocyclone classification.

From a physical standpoint, this approach is particularly meaningful, since the regions where the distributions exhibit the highest divergence correspond to the most sensitive operational ranges for sedimentation and filtration processes. For instance, near the transition boundaries between fine and semi-coarse particles, even small variations in particle structure can lead to significant changes in flocculant consumption or filtration efficiency. Therefore, selecting the point of maximum variance effectively extracts a quantitative and reliable indicator for engineering comparison among mineral samples, enabling more accurate decision-making in the design and optimisation of solid–liquid separation processes.

$$\overline{WDI} = \frac{1}{n}\sum_{i=1}^{n} WDI_i(di) \qquad d_i \text{ calculation loop (2)}$$

$$J(di) = \frac{1}{n}\sum_{i=1}^{n}(WDI_i(di) - \overline{WDI})^2, J'(di) = \frac{2}{n}\sum_{i=1}^{n}(WDI_i(di) - \overline{WDI})WDI_i'(di), optimum\ di\ is\ at\ J'(di) = 0\ and\ J''(di) > 0$$

Based on the data presented in Table 1 and the analytical relations expressed in Equation 2, process threshold diameter for the mineral tailings dataset is estimated as d_i = 76.53 μm. Accordingly, the WDI was identified as the representative particle size metric.

The reference diameter d_i from a methodological and practical standpoint serves as a statistically meaningful metric that summarises particle size behaviour across multiple mineral samples. By identifying the diameter corresponding to the maximum variance of cumulative WDI values among the datasets, this approach effectively highlights the size range where sample differentiation is most pronounced. Mathematically, this is achieved by locating the point where the derivative of the variance function satisfies $J'(di) = 0$ and the second derivative $J''(di) > 0$, ensuring that the selected d_i represents the most discriminative region of the PSD. Physically, these regions typically coincide with the transition boundaries between fine and coarse particle populations, which are critically important for the efficiency of sedimentation, filtration, and hydrocyclone classification. By combining the dual log-normal components into a weighted cumulative WDI,

the method preserves the multi-modal information of the PSD while providing a dimensionless, comparable parameter across samples. Therefore, d_i is not merely a statistical artifact but a quantitative, engineering-relevant threshold that links particle size distribution characteristics directly to practical process performance in mineral processing circuits.

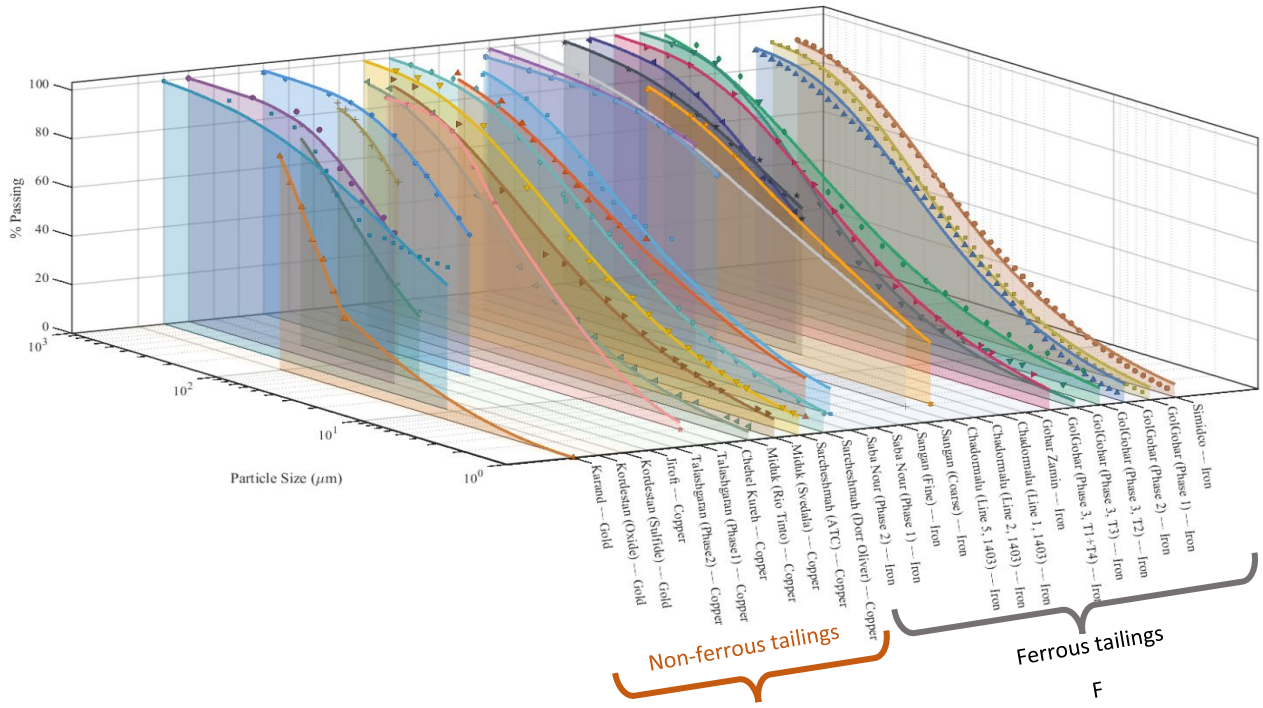

Figure 1 Sieve analysis of tailings particle size distribution and fitted (2) log-normal model curves

Table 1 Fitted 2 log-normal coefficients to the particle size distribution data. WDI = weighted distribution index

Sample	W_1	μ_1	σ_1	W_2	μ_2	σ_2	WDI	Tailing type
Chehel Kureh	0.5	3.296	0.6	0	0	0	0.95875	Copper
Talashgaran (Phase1)	0.5	3.315	1.15	0	0	0	0.813107	Copper
Kordestan (Oxide)	0.5	3.405	1.1	0	0	0	0.801784	Gold
Kordestan (Sulfide)	0.5	3.49	1	0	0	0	0.801729	Gold
Karand	0.5	3.94	0.59	0	0	0	0.749927	Copper and gold
Talashgaran (Phase2)	0.2	4.519	0.541	0.3	0.726	0.91	0.747517	Copper
Miduk (Rio Tinto)	0.25	4.32	0.47	0.25	2.421	1.52	0.705737	Copper
Miduk (Svedala)	0.29	4.276	0.709	0.21	1.876	1.79	0.694651	Copper
Sarcheshmeh (Dorr Oliver)	0.4	2.65	1.78	0.1	4.72	0.366	0.692429	Copper
Sarcheshmeh (ATC)	0.3	2.25	2.1	0.2	4.44	0.68	0.680072	Copper
Talashgaran (Phase1) 15 g/tonne	0.5	3.78	1.256	0	0	0	0.671522	Copper
Talashgaran (Phase1) 22 g/tonne	0.5	4.01	1.256	0	0	0	0.602953	Copper

Sample	W_1	μ_1	σ_1	W_2	μ_2	σ_2	WDI	Tailing type
Talashgaran (Phase1) 28 g/tonne	0.5	4.24	1.256	0	0	0	0.531037	Copper
Jiroft	0.5	4.5	0.85	0	0	0	0.424338	Copper
Ehya Sepahan	0.5	3.32	0.57	0	0	0	0.962921	Iron
Sangan (fine)	0.5	1.4	1.7	0	0	0	0.958017	Iron
Sangan (coarse)	0.5	1.317	2.188	0	0	0	0.916303	Iron
Chadormalu (Line 2, 1403)	0.5	2.5	1.7	0	0	0	0.860166	Iron
Chadormalu (Line 5, 1403)	0.5	2.3	2	0	0	0	0.845876	Iron
Gol Gohar (Phase 2)	0.5	2.85	1.55	0	0	0	0.831442	Iron
Chadormalu (Line 1, 1403)	0.5	3	1.63	0	0	0	0.794104	Iron
Gol Gohar (Phase 3, T1+T4)	0.39	3.7	1.16	0.11	0.06	1.17	0.772824	Iron
Gol Gohar (Phase 1)	0.5	3.318	1.49	0	0	0	0.753151	Iron
Chadormalu (Line 5, 1403) 15 g/tonne	0.5	3.35	1.8	0	0	0	0.708424	Iron
Simidco	0.5	3.4	1.72	0	0	0	0.707206	Iron
Chadormalu (Line 5, 1403) 30 g/tonne	0.5	3.4	1.75	0	0	0	0.703984	Iron
Gohar Zamin	0.5	3.7	1.2	0	0	0	0.702468	Iron
Gol Gohar (Phase 3, T3)	0.39	4.2	0.8	0.11	0.9	2	0.653922	Iron
Gol Gohar (Phase 3, T2)	0.28	2.4	2.4	0.22	4.85	0.75	0.551387	Iron
Saba Nour (Phase 2)	0.5	4.75	0.85	0	0	0	0.313865	Iron
Saba Nour (Phase 1)	0.5	4.737	0.74	0	0	0	0.294791	Iron

The WDI is formulated from a bimodal log-normal distribution to enable consistent and quantitative comparison among samples. This index provides an experimentally grounded numerical measure that integrates the effects of particle size, relative abundance of each size fraction, and process-induced phenomena such as multi-stage grinding, recirculating loads, and the coexistence of coarse and fine particles. As a dimensionless and easily comparable parameter, the WDI establishes a direct correlation with sedimentation and filtration performance across different tailings types. The process threshold diameter is determined through analysis of variance applied to cumulative particle size distributions at varying size intervals, allowing the WDI to function as a unified and statistically validated descriptor of particle size behaviour. Experimental results show that the WDI effectively categorises samples into distinct settling-rate families, with the index decreasing systematically as settling velocity increases. In accordance with prior research on particle size influences, the classification of tailings samples based on WDI values is summarised in Table 2.

Table 2 Weighted distribution index (WDI) classification

Particle size distribution character	WDI range	D_{80} apx.
Coarse dominant tailing (CD)	0.4-0.67	>150 µm
Medium ranged tailing (MR)	0.67-0.75	(75–150 µm)
Fine dominant tailing (FD)	0.75–1.00	<75 µm

3.3 X-ray fluorescence analysis of tailings samples

The chemical composition of the mineral tailings, as illustrated in Figure 2, clearly reveals 2 major categories: non-ferrous tailings, characterised by dominant silica content and reduced iron concentration, and ferrous tailings, which exhibit the opposite trend — lower silica levels and significantly higher iron content.

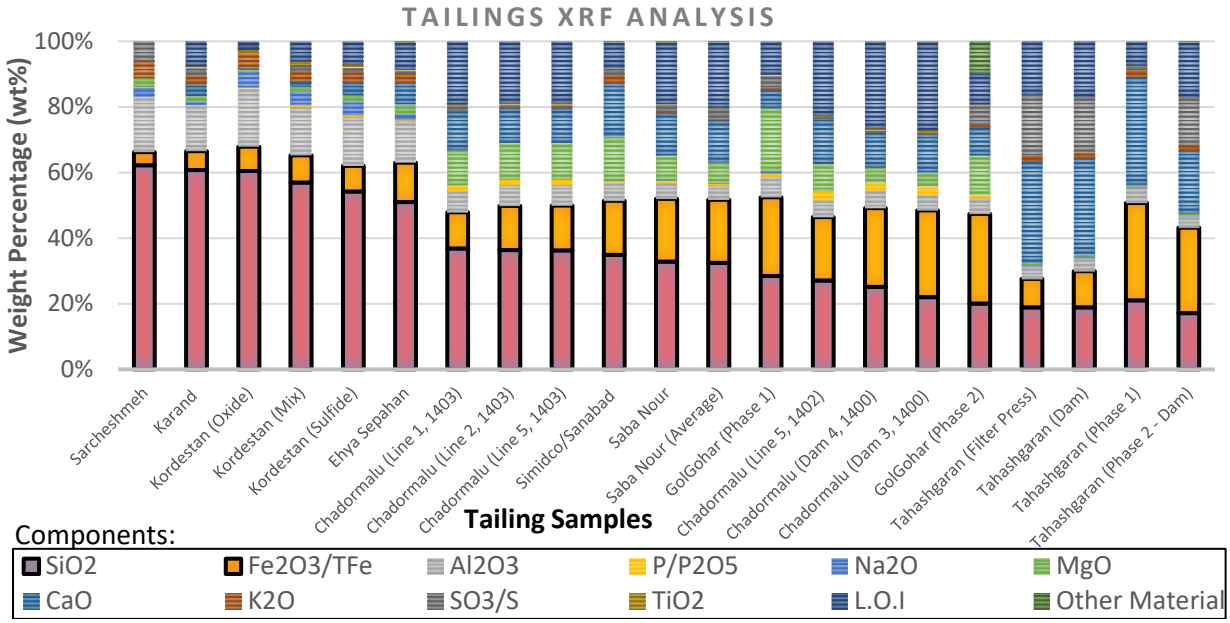

Figure 2 X-ray fluorescence (XRF) analysis of tailing samples

This distinction represents the fundamental classification framework for the chemical grouping of mineral tailings, where the Fe–Si duality largely governs the overall behaviour of the system. In general, non-ferrous tailings contain more than 55 wt% SiO_2 and less than 8 wt% Fe, whereas ferrous tailings show silica contents reduced to 20–37 wt%, with iron concentrations exceeding 20 wt%. This inverse correlation between silica and iron is evident not only in their absolute values but also in their Fe/SiO_2 ratio. For example, in the Sarcheshmeh tailings this ratio is about 0.06, reflecting a strongly siliceous composition, while in Gol Gohar (Phase 2) it reaches 1.35, indicating an iron-dominant regime with minimal silica. This ratio can thus serve as a simple yet effective index for classifying samples into 3 distinct compositional domains: Silica-dominant Zone ($Fe/SiO_2 < 0.2$), Transition Zone (0.2–0.6), Iron-dominant Zone ($Fe/SiO_2 > 0.6$).

The proposed framework assesses the feasibility of a classification map predicting tailings settling and filtration behaviour using only SiO_2 and Fe_2O_3 contents. Silica-rich tailings (quartz, feldspars, aluminosilicate clays) have fine, low-density particles with permanently negative surface charges near neutral pH, resulting in high dispersion stability and low settling rates. Iron-rich tailings (magnetite, hematite, goethite, often with calcite or dolomite) show higher densities, faster settling, and distinct surface-charge behaviour due to higher isoelectric points. Samples with high LOI, CaO, and MgO (e.g. Gol Gohar, Talashgaran) indicate carbonate presence, while other oxides (Al_2O_3, Na_2O, K_2O, TiO_2) have minor background effects; high SO_3 in Talashgaran suggests gypsum or sulphates. A two-dimensional Fe–Si map effectively classifies samples into siliceous, ferruginous, and transition domains, correlating with particle density, zeta potential, and specific surface area, which follow the same compositional trends.

4 Integrated study of sedimentation and filtration with respect to weighted distribution index and chemical composition

4.1 Sedimentation behaviour of ferrous and non-ferrous mineral tailings slurries

The sedimentation experiments are conducted using a 1,000 mL graduated cylinder. As shown in Figure 3, when the sedimentation test results are analysed in combination with the XRF data, a clear correlation emerges between the chemical composition and the dynamic settling behaviour of the tailings. The data indicate that non-ferrous tailings, characterised by high silica and low iron contents, exhibit a gentle initial slope on the settling curves. This behaviour results from the dominance of fine particles with large specific surface area and significant surface charge, which promote colloidal stability and prolong the free-settling phase. In contrast, ferrous tailings show a distinctly different behaviour. Their settling curves display a steep initial slope, with a rapid decrease in slurry height occurring within a short time interval (typically less than one minute). This phenomenon is attributed to the higher particle density, enhanced flocculation, and the formation of denser flocs. In the later stage of the curve, a positive gradient toward lower height values is observed, reflecting the high compressibility of the slurry and the achievement of a high-solids underflow. From an operational standpoint, such behaviour enables the design of thickeners with higher surface loading rates and improved filter press efficiency in industrial applications.

A third group, representing intermediate compositions, exhibits transitional behaviour. In these cases, the initial settling velocity is moderate: although a noticeable height reduction occurs during the first few minutes, the final stabilised height remains higher than that of ferrous tailings. Tests conducted with flocculant addition in the Sarcheshmeh and Chadormalu tailings also confirm that increasing the flocculant dosage up to an optimum concentration reduces the settling time. However, excessive dosing leads to over flocculation (overdose phenomenon) and re-stabilisation of particles, ultimately decreasing the overall performance.

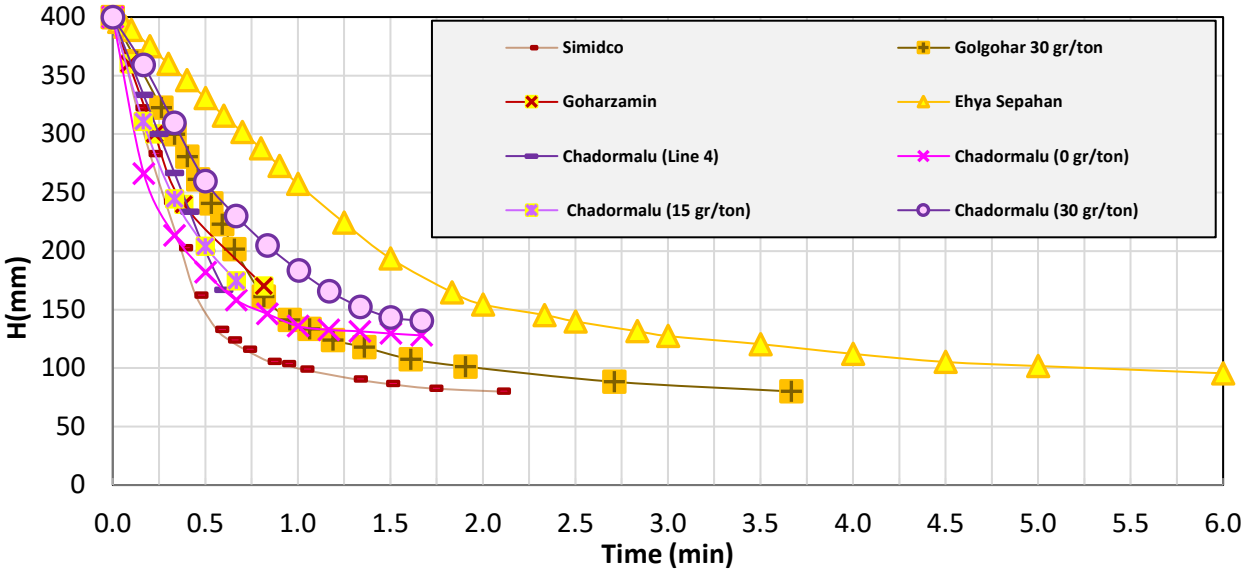

(a)

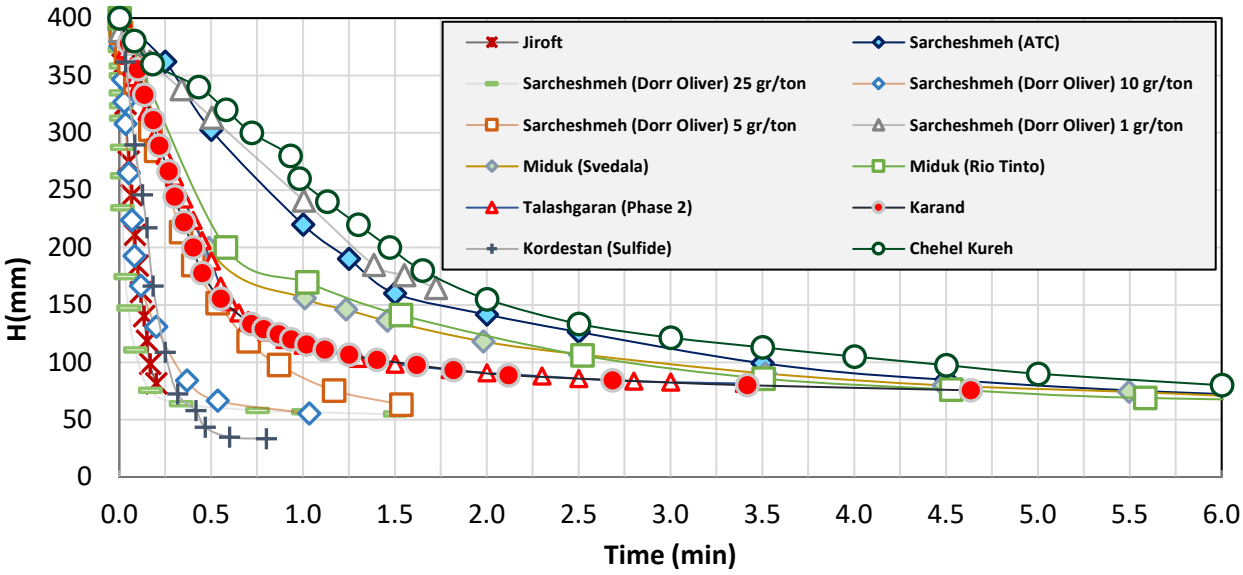

(b)

Figure 3 Sedimentation test results (mudline behaviour). (a) Ferros tailings; (b) Non-ferros tailings

It can be concluded that the settling behaviour of studied mineral tailings is directly influenced by the SiO_2 to Fe_2O_3 (or total Fe) ratio chiefly, leading to 2 dominant behavioural patterns: a siliceous regime characterised by slow settling, bulky tailings and difficult dewatering, and a ferrous regime defined by rapid settling, dense tailings and facilitated dewatering.

A comprehensive understanding of sedimentation behaviour requires analysing both the initial slope, which represents the early-stage settling rate, and the final slope, which reflects tail-end compressibility. These 2 parameters are complementary, and their combined assessment provides a complete basis for designing and optimising solid–liquid separation systems in mineral processing. As shown in Table 3 and Figure 4, the sedimentation behaviour of mineral tailings is governed by the interaction between chemical composition (mainly SiO_2 and Fe compounds) and the WDI. A lower WDI, indicating coarser particle fractions, correlates with steeper initial slopes and faster settling. Within the WDI range of 0.40–0.67, coarse silica promotes sedimentation through 3 mechanisms: its larger grain size increases settling velocity per Stokes' law, a ballasting effect develops as coarse particles drag finer ones downward, and reduced surface-to-volume ratio

weakens electrostatic repulsion and enhances floc formation. Thus, in this regime, silica acts as a sedimentation promoter. In the intermediate WDI range (0.67–0.75), settling rates become moderate and are controlled by a combined Fe–Si influence – higher Fe content increases particle density and floc compactness, while elevated SiO_2 (30–40 wt%) strengthens surface charge and colloidal stability, reducing settling. This coupled zone is highly sensitive to flocculant type and dosage, making it a key operational window for process optimisation.

For fine particles (corresponding to high WDI values) the initial slope of the sedimentation curves decreases sharply, indicating very slow settling. In this regime, fine-grained silica acts as a strong inhibitor due to its high specific surface area, strong colloidal stability, and formation of gel-like networks that restrict fluid drainage, leading to elongated sedimentation tails and higher slurry viscosity. The contrast between ferrous and non-ferrous tailings further highlights these trends: Fe-rich systems (e.g. Gol Gohar, Chadormalu) settle rapidly and exhibit high compressibility owing to the greater density and surface reactivity of iron oxides, whereas Si-rich systems (e.g. Sarcheshmeh, Karand) are dominated by fine silica particles that slow settling. Overall, tailings settling depends on particle size, chemical composition, and ore type – accelerated by coarse silica, hindered by fine silica, and balanced by the Fe/Si ratio in intermediate cases. These findings are vital for optimising thickener and filtration design, emphasising the need to evaluate both initial (free-settling) and final (compressive) slopes to develop an integrated model for solid–liquid separation and tailings management.

Table 3 Analysis of settling curve slopes as a function of weighted distribution index (WDI), Si/Fe compositions

Sample	Weighted distribution index	Fe (%)	Si (%)	Initial slope (mm/sec)	Final slope (mm/sec)	Tailing type	Particle size distribution character
Jiroft	0.424338	18.5	60.21	−38.60	−0.05	Copper	CD
Talashgaran (Phase1) 28 g/tonne	0.531037	26.64	18.85	−26.29	−0.07	Copper	CD
Kordestan (Sulfide)25 g/tonne	0.593987	7.85	54.1	−19.97	−0.1	Gold	CD
Talashgaran (Phase1) 22 g/tonne	0.652428	26.64	18.85	−16.80	−0.29	Copper	CD
Talashgaran (Phase2) Dam	0.747517	28.62	18.88	−10.59	−0.30	Copper	MR
Talashgaran (Phase1) 15 g/tonne	0.671522	26.64	18.85	−8.98	−0.15	Copper	MR
Karand	0.749927	5.57	60.7	−8.66	−0.4	Gold and copper	MR
Miduk (Svedala)	0.694651			−6.87	−0.55	Copper	MR
Miduk (Rio Tinto)	0.705737			−5.75	−0.62	Copper	MR
Talashgaran (Phase1)	0.813107	26.64	18.85	−4.93	−0.70	Copper	FD
Chehel Kureh	0.95875			−4.17	−1.253	Copper	FD
Sarcheshmah (ATC)	0.680072	3.99	62.24	−2.84	−1.39	Copper	FD
Sarcheshmah (Dorr Oliver)	0.692429	5.26	63.09	−2.56	−1.47	Copper	FD
Chadormalu (Line 5, 1403) 30 g/tonne	0.679865	13.57	36.31	−13.29	−0.16	Iron	CD
Simidco	0.707206	16.49	34.89	−9.35	−0.25	Iron	MR
Chadormalu (Line 5, 1403) 15 g/tonne	0.708424	13.57	36.31	−9.05	−0.17	Iron	MR
Gohar Zamin	0.702468			−7.57	−0.10	Iron	MR
Chadormalu (Line 2, 1403)	0.860166	13.55	36.33	−6.66	−0.01	Iron	MR
Gol Gohar (Phase 1)	0.753151	28.42	24.02	−5.27	−0.50	Iron	MR
Chadormalu (Line 5, 1403)	0.845876	13.57	36.31	−4.30	−0.84	Iron	FD
Ehya Sepahan	0.962921	11.99	50.91	−1.96	−1.50	Iron	FD

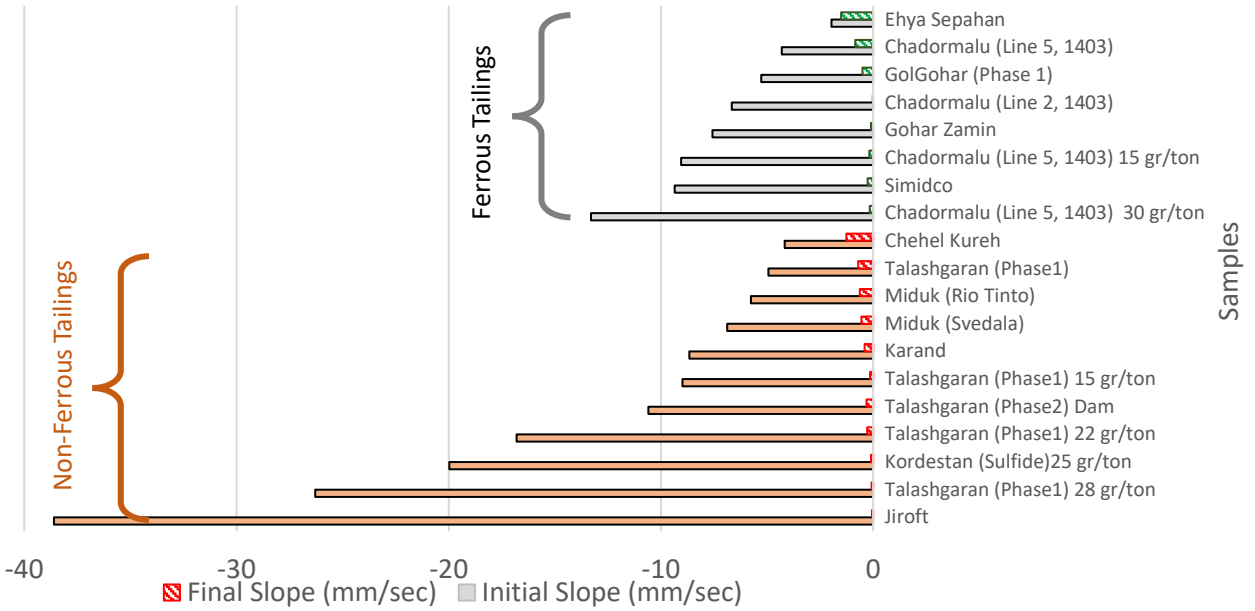

Figure 4 Tailing samples sedimentation behaviour (initial and final slope chart)

Examination of Table 3 indicates a general and quantitative correspondence between Fe–Si content and WDI. Samples with relatively higher Fe/Si ratios and lower WDI values (WDI < 0.67) tend to exhibit steeper initial settling slopes (|slope| ≈ 9–39 mm/s), consistent with coarse dominant tailings, whereas silica-rich samples (Si > 50 wt%) with higher WDI (> 0.75) generally fall within the fine dominant domain and show slower settling rates (|slope| < 5 mm/s). This observation can be approximately captured by a first-order relation, $|S_0| \sim (Fe/Si)\cdot(1-WDI)$, providing a tentative quantitative link between chemical composition, particle size distribution, and settling behaviour. This empirical relation provides a preliminary roadmap for linking Fe–Si composition with tailings settling rates and filtration performance, which can be refined through data sharing and standardisation.

4.2 Ferrous and non-ferrous mineral tailing filtration

The filtration test data, along with their associated result ranges, are presented in Figure 5. For consistent comparison of filtration performance, the main dependent variable is defined as the mass of filtrate collected per unit chamber volume, representing the overall filtration efficiency, and is also illustrated in Figure 6. With decreasing WDI, the initial dewatering rate consistently rises, showing a direct correlation with permeability theory. The presence of coarser particles promotes the formation of micro-channels within the cake, resulting in higher effective porosity and thus an increased effective permeability coefficient (k). This trend is also consistent with the Kozeny–Carman equation ($k \propto d_P^2 \frac{\varepsilon^3}{(1-\varepsilon)^2}$).

Additionally, coarse particles are less susceptible to pore blockage by fine fillers, resulting in smoother initial flow and greater water removal. Nevertheless, dewatering efficiency is not solely controlled by PSD; mineralogy, compressibility, and entrapped water also play major roles. Silica-rich tailings, characterised by high specific surface area, strong surface adhesion, and extensive pore filling, retain more water and exhibit lower permeability and filtrate yield – behaviour observed in the Chadormalu (Line 5), Kordestan, and Karand samples, which deviate from the general WDI–dewatering trend. In contrast, iron-rich tailings produce higher filtrate volumes due to their hard, dense, non-platy, and nearly spherical particles, which promote efficient drainage and result in lower residual moisture.

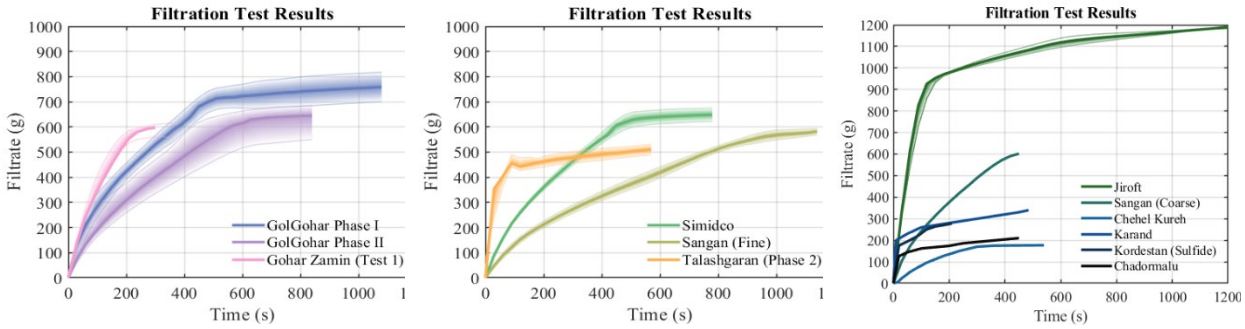

Figure 5 Filtration test results of mineral slurries including laboratory result ranges. (a) Gol Gohar and Gohar Zamin samples; (b) Simidco, Sangan and Talashgaran samples; (c) Jiroft, Sangan, Chehel Kureh, Karand, Kordestan and Chadormalu samples

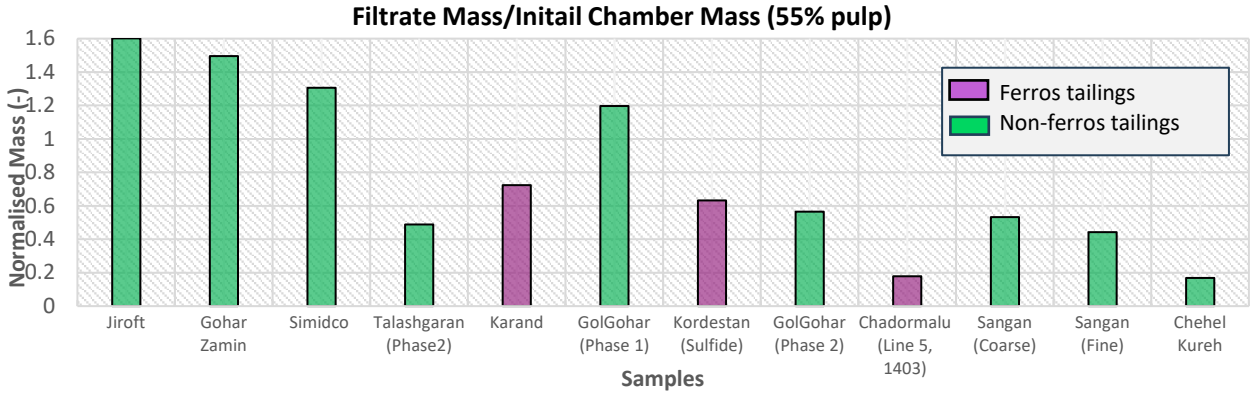

Figure 6 The dimensionless ratio of final filtrate mass to the initial slurry mass in the chamber

5 Integrative conclusions on sedimentation and filtration

The results of this study demonstrate that the sedimentation and filtration behaviour of mineral tailings is controlled by both physical and chemical properties, with particle size distribution and the relative proportions of iron- and silica-bearing phases exerting strongest influence. Iron-rich tailings, containing higher Fe_2O_3 and coarser particles, exhibit faster settling, greater compressibility, and better dewaterability, while siliceous tailings, dominated by fine, high–surface-area particles, show strong colloidal stability and poor water release. These contrasts arise from differences in density, surface charge, and microstructure, which jointly determine slurry rheology and cake permeability. The Fe-Si ratio thus serves as a reliable predictor of dewatering performance. Laboratory data further reveal that iron-bearing particles consistently enhance settling, whereas silica exerts a dual effect, promoting it in coarse fractions but hindering it in fine ones. Quantified through the WDI, this relationship provides a general framework for analysing sedimentation and filtration in other tailings systems. From a processing perspective, coarse particles form larger, more permeable pore networks that increase filtration rate and reduce moisture, while fine or platy particles clog pores and raise specific resistance. Therefore, optimising dewatering conditions requires accounting for both the true PSD and the representative particle diameter of each tailings type.

Ultimately, this study introduces the WDI and the Fe–Si compositional index as quantitative criteria for evaluating and comparing the dewatering potential of mineral tailings. These metrics enable a systematic assessment of the combined effects of particle size and chemistry on sedimentation–filtration behaviour and can serve as a foundation for developing predictive models and machine-learning algorithms for dewatering system design. This study enables plant operators to anticipate changes in dewatering and filtration performance under variable feed conditions, while offering process designers a practical framework for assessing and improving the adaptability of unit operations to feed variability at different scales.

Acknowledgement

The authors would like to extend their profound appreciation to all Iranian mining companies for their cooperation and for providing access to the data utilised in this study, in particular Simidco, Gol Gohar, Nicico, and Doryaban Companies. The authors are also sincerely grateful to Mr Pourkhadem, Mr Ardeshiri, Mr Shahid Sales, and Mr Rostami for their insightful comments, valuable guidance, and continuous support throughout the course of this research.

References

Cacciuttolo Vargas, C & Pérez Campomanes, G 2022, 'Practical experience of filtered tailings technology in Chile and Peru: an environmentally friendly solution', *Minerals*, vol. 12, no. 7, https://doi.org/10.3390/min12070889

Diaz, A, Ahmed, I, Kerry, P, Corrigan, P & Stewart, F 2023, 'Filtered tailings plant design at Krumovgrad Mine', in GW Wilson, NA Beier, DC Sego, AB Fourie & D Reid (eds), *Paste 2023: Proceedings of the 25th International Conference on Paste, Thickened and Filtered Tailings*, Australian Centre for Geomechanics, Perth, pp. 316–323, https://doi.org/10.36487/ACG_repo/2355_24

Ferreira, D, Fiuza, M, Cardoso, M & Oliveira, I 2021, 'Use of the Weibull model on sizing thickeners-part I: sedimentation curve representation', *The Canadian Journal of Chemical Engineering*, vol. 99, no. 3, pp. 708–724.

Fränkle, B, Sok, T, Gleiß, M & Nirschl, H 2022, 'Iron ore tailings dewatering: measurement of adhesion and cohesion for filter press operation', *Sustainability*, vol. 14, no. 6, https://doi.org/10.3390/su14063424

Fränkle, B, Sok, T, Gleiß, M & Nirschl, H 2024, 'Copper tailings filtration: Influence of filter cake desaturation', *Minerals Engineering*, vol. 217, https://doi.org/10.1016/j.mineng.2024.108952

Han, C, Tan, Y, Chu, L, Song, W & Yu, X 2022, 'Flocculation and settlement characteristics of ultrafine tailings and microscopic characteristics of flocs', *Minerals*, vol. 12, no. 2, https://doi.org/10.3390/min12020221

Hassan, S, Cavalida, R, Ekanayake, NI, Scales, PJ, Batterham, RJ & Stickland, AD 2025, 'High pressure dewatering rolls Mark-II: a novel dewatering technology for mineral tailings', *Minerals Engineering*, vol. 232.

Hernández, CA, Pizarro, EA, Molina, JA, de Araujo, AC & Valadão, GES 2009, 'Mineral paste comparison between copper and iron tails', in R Jewell, AB Fourie, S Barrera & J Wiertz (eds), *Paste 2009: Proceedings of the Twelfth International Seminar on Paste and Thickened Tailings*, Australian Centre for Geomechanics, Perth, pp. 47–55, https://doi.org/10.36487/ACG_repo/963_6

Kaswalder, F & Hawkey, A 2023, 'Filter cake desaturation: a laboratory-scale study of two copper sulphide flotation tailings slurries dewatered in a filter press', *Alta 2023*.

Li, Y & van Zyl, D 2024a, 'Analysing the segregation of coarse tailings particles with a zone-formation differential settling model', in AB Fourie & D Reid (eds), *Paste 2024: Proceedings of the 26th International Conference on Paste, Thickened and Filtered Tailings,* Australian Centre for Geomechanics, Perth, pp. 271–282, https://doi.org/10.36487/ACG_repo/2455_22

Li, y & D, van Zyl 2024b, 'Experimental study on the overall settling behaviour of copper tailings suspension', *Minerals Engineering*, vol. 218, https://doi.org/10.1016/j.mineng.2024.108580

Luo, Y, Ekanayake, N, Amini, N, Moon, E, Hapgood, K, Scales, P & Stickland, A 2024, 'Quantifying the effects of clays on mineral tailings filtration', *Minerals Engineering*, vol. 216, https://doi.org/10.1016/j.mineng.2024.108830

Nupehewa, J, Palmer, J, Suvio, P, Koponen, V & Safonov, D 2023, 'Developing predictive empirical filtration models for advanced tailings handling', in GW Wilson, NA Beier, DC Sego, AB Fourie & D Reid (eds), *Paste 2023: Proceedings of the 25th International Conference on Paste, Thickened and Filtered Tailings*, Australian Centre for Geomechanics, Perth, pp. 324–338, https://doi.org/10.36487/ACG_repo/2355_25

Olcay, RH, Ordóñez, S, Valadão, G, Patiño, F, Henriques, H, Reyes, I & Flores, M 2025, 'Industrial-scale application of polymer dewatering for fine tailings disposal', *Materials*, vol. 18, no. 16, https://doi.org/10.3390/ma18163872

Paoli, Í & da Silveira, VW 2023, 'Study of the sedimentation parameters of an iron ore tailing from Fundão Dam using a tannin-based coagulant', *Mining*, vol. 3, no. 2, pp. 224–229, https://doi.org/10.3390/mining3020013

Pham, H 2005, *Particles in Water: Properties and Processes*, 1st edn, CRC Press, Boca Raton, https://doi.org/10.1201/9780203508459

Pham, H, Pham, P, Tien, T, Phung, D & Vu, C 2024, 'Research on the factors affecting the product filtration efficiency in mineral processing plants', *Journal of Mining and Earth Sciences*, vol. 62, no. 2, pp. 76–85.

Sadangi, J, Sahoo, A, Sushobhan, B & Choudhury, N 2020, 'Effect of anionic flocculant on settling rate of iron ore ultra-fines', *Materials Today: Proceedings*, vol. 30, pp. 316–321, https://doi.org/10.1016/j.matpr.2020.01.594

Tan, Y, Han, C, Chu, L, Song, W & Yu, X 2022, 'Research on flocculant selection for classified fine tailings based on micro-characterization of floc structure characteristics', *Materials*, vol. 15, no. 7, https://doi.org/10.3390/ma15072460

Tchobanoglus, G, Burton, F & Stensel, H 2003, 'Wastewater engineering: treatment and reuse', *American Water Works Association*, vol. 95, no. 5.

Wang, J, Du, Z, Liu, X & Wu, A 2025, 'Experimental study on the thickening characteristics of ultrafine tailings', *Minerals*, vol. 15, no. 2, https://doi.org/10.3390/min15020100